Am J Physiol Renal Physiol 294: F53–F61, 2008.
First published October 10, 2007; doi:10.1152/ajprenal.00314.2007.

Intracellular targeting of copper-transporting ATPase ATP7A in a normal and *Atp7b*$^{-/-}$ kidney

Rachel Linz,[1]* Natalie L. Barnes,[1]* Adriana M. Zimnicka,[2] Jack H. Kaplan,[2] Betty Eipper,[3] and Svetlana Lutsenko[1]

[1]*Department of Biochemistry and Molecular Biology, Oregon Health and Science University, Portland, Oregon;* [2]*Department of Biochemistry and Molecular Genetics, University of Illinois, Chicago, Illinois; and* [3]*Department of Neuroscience, University of Connecticut Health Center, Farmington, Connecticut*

Submitted 9 July 2007; accepted in final form 9 October 2007

Linz R, Barnes NL, Zimnicka AM, Kaplan JH, Eipper B, Lutsenko S. Intracellular targeting of copper-transporting ATPase ATP7A in a normal and *Atp7b*$^{-/-}$ kidney. *Am J Physiol Renal Physiol* 294: F53–F61, 2008. First published October 10, 2007; doi:10.1152/ajprenal.00314.2007.—Kidneys regulate their copper content more effectively than many other organs in diseases of copper deficiency or excess. We demonstrate that two copper-transporting ATPases, ATP7A and ATP7B, contribute to this regulation. ATP7A is expressed, to a variable degree, throughout the kidney and shows age-dependent intracellular localization. In 2-wk-old mice, ATP7A is located in the vicinity of the basolateral membrane, whereas in 20-wk-old mice, ATP7A is predominantly in intracellular vesicles. Acute elevation of serum copper, via intraperitoneal injection, results in the in vivo redistribution of ATP7A from intracellular compartments toward the basolateral membrane, illustrating a role for ATP7A in renal response to changes in copper load. Renal copper homeostasis also requires functional ATP7B, which is coexpressed with ATP7A in renal cells of proximal and distal origin. The kidneys of *Atp7b*$^{-/-}$ mice, an animal model of Wilson disease, show metabolic alterations manifested by the appearance of highly fluorescent deposits; however, in marked contrast to the liver, renal copper is not significantly elevated. The lack of notable copper accumulation in the *Atp7b*$^{-/-}$ kidney is likely due to the compensatory export of copper by ATP7A. This interpretation is supported by the predominant localization of ATP7A at the basolateral membrane of *Atp7b*$^{-/-}$ cortical tubules. Our results suggest that both Cu-ATPases regulate renal copper, with ATP7A playing a major role in exporting copper via basolateral membranes and protecting renal tissue against copper overload.

ATP7B; Wilson disease; basolateral membrane; trafficking

COPPER PLAYS AN ESSENTIAL ROLE in mammalian physiology. It is required as a cofactor for key metabolic enzymes including cytochrome *c* oxidase, tyrosinase, lysyl oxidase, peptidylglycine α-amidating monooxygenase, Cu,Zn-superoxide dismutase, and others. However, excess copper can be toxic, and maintenance of copper balance in cells is critical. Two copper-transporting P-type ATPases (Cu-ATPases), ATP7A and ATP7B, play a central role in this process. Cu-ATPases have dual functions in the delivery of copper to cuproenzymes in the *trans*-Golgi network (TGN) and in exporting excess copper from the cell. Inactivation of either ATP7A or ATP7B in humans results in severe metabolic disorders, Menkes disease and Wilson disease, respectively. Menkes disease is characterized by defective copper transport from the enterocytes into the circulation and is associated with severe copper deficiency in several tissues, particularly in the brain. In Wilson disease, copper export from the liver into the bile is disrupted, resulting in marked copper overload in the liver. Although phenotypic manifestations of the two diseases are very different, both Menkes disease and Wilson disease result in copper accumulation in kidneys (3, 22). This observation suggests that both ATP7A and ATP7B are necessary for normal renal copper balance. Currently, the specific contribution of each Cu-ATPase to renal copper metabolism is poorly understood.

Renal copper content is among the highest in the body (15) and is tightly regulated. In dietary deficiency or in a situation when intestinal copper absorption is greatly diminished due to genetic inactivation of the copper uptake protein CTR1, the kidney copper content appears less affected compared with other tissues (23, 28). This is also the case in Menkes disease, where defective copper export from the intestine results in copper deficiency in most other tissues, yet copper levels in the kidney rise above that of healthy individuals (22). In patients with Wilson disease patients and in mouse models, copper is markedly elevated in the liver at a young age, whereas renal copper rises more slowly (1, 3, 4), suggesting a more precise control of renal copper content. This tighter control could be, at least partially, due to the presence of two (rather than one) Cu-ATPases, and it may involve fine-tuned cross talk between ATP7A and ATP7B. Currently, the information on the localization and function of ATP7A and ATP7B in kidney is very limited.

Recent studies of the expression and localization of ATP7A and ATP7B in the kidney have yielded inconsistent results. In situ hybridization of ATP7A mRNA in the mouse kidney showed strong staining in proximal tubules (19), in contrast to another study in which the glomerulus showed the strongest staining and proximal tubules were stained weakly (17). In immunochemistry experiments using control and brindled mice (an animal model of Menkes disease), ATP7A was detected in the proximal and distal tubules but not in the glomerulus (6). In a study of transgenic mice overexpressing human ATP7A, two transgenic strains showed different patterns of ATP7A expression in kidney, which included distal tubules, the loops of Henle, outer medulla, and the podocytes of the glomerulus, but no expression in proximal tubule (9). No staining of the transgene product was seen in the proximal tubules. ATP7B distribution was investigated only in one study, and both mRNA and protein were found in the glomerulus and inner and outer medulla (17).

* R. Linz and N. L. Barnes contributed equally to this work.
Address for reprint requests and other correspondence: S. Lutsenko, Oregon Health & Science Univ., Portland, OR 97239 (e-mail: lutsenko@ohsu.edu).

The costs of publication of this article were defrayed in part by the payment of page charges. The article must therefore be hereby marked "*advertisement*" in accordance with 18 U.S.C. Section 1734 solely to indicate this fact.

The discrepancies in the reported localization of Cu-ATPases could be due to varying animal strains and ages as well as the detection of mRNA compared with protein. To date, no developmental studies of Cu-ATPase in the kidney have been reported. Similarly, the effects of altered copper levels on endogenous Cu-ATPases in the kidney remain unknown. It was previously reported that recombinant ATP7A, when expressed in Madin-Darby canine kidney (MDCK) cells, undergoes trafficking from the intracellular vesicles to the basolateral membrane in response to high extracellular copper (5). Whether changes in serum copper have any effect on endogenous ATP7A in vivo has not been investigated. To begin addressing these important issues, we performed high-resolution immunohistochemical mapping of endogenous ATP7A in the tubular epithelial cells of mouse kidney. Our studies revealed a widespread distribution of ATP7A in kidney and demonstrated that the intracellular localization of endogenous ATP7A is age-dependent and can be modulated in vivo by changes in serum copper or by inactivation of another copper-transporting ATPase, ATP7B. Altogether, our results support the role of ATP7A in copper export across the basolateral membrane for reabsorption into the blood; in addition, they provide a direct demonstration of a cross talk between the two renal copper-transporting ATPases.

METHODS

Mice. The generation of *Atp7b*$^{-/-}$ mice has been described previously (4). The *Atp7b*$^{-/-}$ and wild-type C57BLx129S6/SvEv mice were all housed at the Oregon Health and Science University (OHSU) Department of Comparative Medicine according to the National Institute of Health guidelines on the use of laboratory and experimental animals. The experimental protocol was approved by the OHSU Institutional Animal Care and Use Committee. Food and water were provided ad libitum. Mice of either sex were used. To manipulate serum copper levels, two independent experiments were performed, which showed the same results. In each experiment, two control and two *Atp7b*$^{-/-}$ mice were injected intraperitoneally with 10 μg Cu/g body wt, using $CuCl_2$ in a 0.9% NaCl solution. The 0.9% NaCl solution without copper was used as a negative control. Four hours after injection, mice were euthanized using CO_2 inhalation, and tissues were harvested and processed for immunostaining.

Antibodies and peptides. Primary antibody α-C-Mnkp CT77 was previously described (29). This antibody is directed against a short, COOH-terminal peptide of mouse ATP7A, D1475–L1492. The secondary goat anti-rabbit IgG antibody conjugated to Cy3 was obtained from Molecular Probes (Eugene, OR). To determine specificity of immunostaining by CT77, two recombinant peptides were generated, expressed in *Escherichia coli*, purified, and used for preabsorption experiments. The "specific" competing peptide C-Mnkp corresponded to Y1410–L1501 of human ATP7A, and the "nonspecific" competing peptide C-Wndp corresponded to the Y1376–L1465 fragment of ATP7B. Both peptides, which share ~55% sequence identity, are 12.5 kDa in size with a 6-His tag.

Fluorescent immunohistochemistry. Mice were euthanized by CO_2 inhalation and subjected to transcardial perfusion with a 0.9% NaCl solution followed by a solution of 4% paraformaldehyde (PFA) in phosphate-buffered saline (PBS), pH 7.4. Kidneys were quickly removed and fixed in 4% PFA for 24 h at 4°C and then soaked in 20% sucrose overnight at 4°C. The kidneys were embedded in Tissue-Tek O.C.T. compound (Sakura FineTechnical, Tokyo, Japan) at −20°C and then sectioned into 20-μm sagittal slices using a Leitz Cryostat (Wetzlar, Germany). The slices were placed onto gelatin/poly-L-lysine-coated slides and stored at −80°C. Kidney sections were taken from three animals for each category and each age group.

Slides were warmed to room temperature, and kidney sections were rehydrated with PBS for 5 min. Sections were blocked with 5% goat serum, 1% BSA, and 0.2% Triton X-100, in PBS, for 1 h at room temperature (RT). After a brief rinse in PBS, slides were incubated in the primary antibody (CT77 at 1:2,000) in dilution buffer (DB: 0.25% BSA and 0.2% Triton X-100, in PBS) for 2 h at RT. Slides were washed three times for 10 min in PBS and then incubated in the secondary antibody (Alexa Fluor 555 goat anti-rabbit IgG diluted 1:3,000) in DB for 1 h in the dark. After three more 10-min washes in PBS, slides were mounted using Vectashield with 4′,6-diamidine-2-phenylindole (Vector Labs, Burlingame, CA) and analyzed using a Zeiss LSM5 scanning confocal microscope (Carl Zeiss, Jena, Germany). To determine signal specificity, the CT77 antibody was incubated with 150 μg of C-Mnkp or C-Wndp for 1 h at 4°C before being diluted in DB, and the mixture was then added to slides. Experiments were repeated at least three times, and a minimum of five images per sample were analyzed to determine the most representative staining patterns.

Cell lines. All cultured cell lines were from American Type Culture Collection (Manassas, VA). MDCK and opossum kidney (OK) cells were maintained in Eagle's minimum essential medium (GIBCO, Grand Island, NY) supplemented with 10% fetal bovine serum (GIBCO), 2 mM L-glutamine (GIBCO), 1.5 g/l sodium bicarbonate, 0.1 mM nonessential amino acids, 1.0 mM sodium pyruvate (Invitrogen, Carlsbad, CA), and 100 U/ml penicillin and streptomycin (Invitrogen).

Copper measurements. Blood was collected from animals during transcardial perfusion. After the right atrium was cut open, blood was allowed to drain into the thoracic cavity and was collected before the 0.9% saline solution was injected into the left ventricle. The blood was allowed to clot and was subsequently centrifuged twice for 5 min at 8,000 rpm. Serum was decanted and frozen at −80°C. Freshly removed kidneys were bisected sagittally, and cortex and medulla were dissected; renal pelvis was discarded. Digestion of tissue was done using the wet ashing protocol described by Parker et al. (26). Briefly, the samples were heated under reflux in 0.5 ml of concentrated HNO_3 (~69.5%; Mallinckrodt Baker, Phillipsburg, NJ) for 45 min, cooled to room temperature, transferred to a graduated cylinder, and diluted with water to yield 10 ml (acid concentration ~3.5%).

Atomic absorption measurements were carried out using an AA6650 spectrometer equipped with a graphite furnace and ASC6100 autosampler (Shimadzu, Kyoto, Japan). Samples (both serum and digested tissue samples) were diluted with 2% HNO_3 to be in the linear absorption range of the calibration curve [1–10 parts per billion (ppb, or ng/l)]. Each sample (20 μl) was injected two to three times depending on the standard deviation of measurements. The copper concentration was derived by comparing the absorption of the sample with that of a standard curve. Standard deviations were calculated to reflect the variance in the measurements. All values are expressed as means ± SD.

RESULTS

ATP7A is located throughout the nephron in adult kidney. The localization of renal ATP7A was first examined using immunohistochemistry and confocal microscopy of adult (6–8 wk) kidneys. ATP7A was found to be expressed throughout the kidney and was detected in epithelial cells of renal cortical tubules and tubules of outer and inner medulla, with little to no expression in the renal pelvis (Fig. 1*A*, red). It is apparent that the expression of ATP7A, although widespread, is uneven along the nephron, with some tubules exhibiting bright staining and others showing low levels of ATP7A (Fig. 1*B*). Higher magnification images show that the podocytes of the glomeruli have little, if any, ATP7A; however, epithelial cells of tubules in the immediate vicinity of glomeruli are brightly stained (Fig.

1*B*, pink). Previously, significant discrepancies in the distribution of ATP7A have been reported (see Introduction). Our data agreed with some reports (6, 19) but contradicted others (17); consequently, we investigated the possible reasons for such discrepancies in more detail.

It should be noted that kidneys show significant autofluorescence (Fig. 1*C*). This fluorescence is observed in a wide range of wavelengths, including those used for detection of ATP7A, and it has a punctate intracellular pattern. When fluorescently labeled secondary antibodies were utilized for detection of ATP7A, the intense punctate pattern of autofluorescence could be mistaken for specific intracellular immunostaining. To distinguish autofluorescence from specific staining of ATP7A, we collected images at two different wavelengths: outside of the absorption range of the secondary antibody (where we only detected autofluorescence, Fig. 1*C*, *middle*) and within the absorption range of the secondary antibody (where we detected both specific staining by CT77 and autofluorescence, Fig. 1*C*, *right*). Overlaying the two images separates autofluorescence (which shows overlap at the 2 wavelengths, Fig. 1*C*, *left*, white spots) from specific staining (Fig. 1C, *left*, pink spots). We utilized this approach for most of the images.

To further verify the specificity of immunostaining, the anti-ATP7A antibody (CT77) was preincubated with the purified recombinant peptide corresponding to the COOH-terminal fragment of ATP7A (C-Mnkp), which contains the epitope for CT77. For a negative control, we used the recombinant COOH-terminal fragment of ATP7B (C-Wndp), which is 55% identical to the C-Mnkp peptide but differs in the epitope region. When blocked with the C-Mnkp peptide, CT77 antibody no longer produced the staining and only a faint haze remained (Fig. 1*D*, *middle*). Blocking with the C-Wndp peptide had no significant effect on the immunofluorescent pattern (Fig. 1*D*, *right*), confirming the specificity of ATP7A staining seen with CT77 (Fig. 1*D*, *left*).

Intracellular localization of ATP7A is age dependent. The variable intensity of staining along the nephron that we observed in our experiments and differing patterns previously reported for mice of different ages (10 and 60 days) prompted us to examine whether the expression and distribution of ATP7A in kidney could change during kidney maturation. In general, the localization of a Cu-ATPase at the basolateral membrane of epithelial cells (a membrane facing the blood) would be consistent with its role in exporting copper back into circulation (reabsorption). By contrast, the presence at the apical membrane (the interior portion of renal tubules) would suggest a role for Cu-ATPase in transporting copper into the lumen of tubules for removal of excess copper with urine. Intracellular staining would be consistent with the role in the biosynthesis of cuproproteins and/or copper storage function.

To determine whether the distribution (and presumably function) of ATP7A changes as kidney mature, we compared the ATP7A staining in kidneys of 2-, 8-, and 20-wk-old mice. These experiments yielded very interesting results (Fig. 2). The overall intensity and distribution of ATP7A in renal tissue appeared similar in animals at these three ages, suggesting a lack of considerable fluctuation in protein abundance during kidney maturation or with age. At the same time, there was a very clear age-dependent difference in the intracellular localization of ATP7A (Fig. 2). In 2-wk-old kidneys, epithelial cells of many cortical tubules showed staining of ATP7A close to or at the basolateral membrane (Fig. 2, *left*). In the cortex of 8-wk-old kidneys, some tubules showed basolateral staining in their epithelial cells, while in other tubules the localization of ATP7A was mostly vesicular and perinuclear (Fig. 2, *middle*). The intracellular perinuclear staining became predominant in 20-wk-old animals (Fig. 2, *right*). The ATP7A staining in the medulla was mostly perinuclear in both young and adult mice (data not shown).

Changes in serum copper concentration affect the intracellular localization of ATP7A in vivo. In vitro, the intracellular localization of ATP7A can be altered by treating cells with elevated copper. In response to copper increase, ATP7A traffics from the TGN toward the plasma membrane (13, 24, 5); this step is thought to result in the export of copper from the cell. Consequently, we hypothesized that the dual localization of endogenous ATP7A in tissues (in proximity to the basolateral membrane and in the intracellular vesicles) may reflect the ability of ATP7A to traffic in vivo depending on cellular copper levels. To test this hypothesis, we first examined whether the predominant localization of ATP7A at the basolateral membrane in 2-wk-old kidneys is associated with the increased levels of copper in tissue.

Analysis of tissue (5–7 animals per age group) demonstrated that copper levels in either cortex or medulla of 2-wk-old kidney were not elevated compared with those of older animals (Fig. 3*A*). In the cortex of 2-wk-old kidney, where the localization of ATP7A at the basolateral membrane was the most apparent, the copper concentration in tissue was similar or even slightly lower compared with that in the 8-wk-old samples (3.72 ± 1.17 vs. 4.59 ± 0.34 ppb), but clearly not higher (see also Fig. 3*A*). This result ruled out the high steady-state levels of copper in tissue as a reason for ATP7A relocalization toward basolateral membrane. Alternatively, it seemed possible that in younger animals, serum copper levels could be higher, and hence more copper could be entering epithelial cells from the serum. In this scenario, an increase in copper levels would induce the relocalization of ATP7A toward basolateral membrane, stimulate copper export, and consequently decrease copper levels in tissue. To examine whether more copper is present in the serum of younger mice, we compared copper concentrations in the serum of 2- and 8-wk-old animals, using 6–9 mice for each age group. These measurements did not lend sufficiently strong support to the hypothesis. Although serum copper was on average higher in the 2-wk-old mice compared with the 8-wk-old animals (161.02 ± 37.29 and 144.61 ± 25.59 ppb, respectively), this difference was not statistically significant due to large animal-to-animal variation of values (Fig. 3*B*).

Since natural variations between animals precluded an unambiguous conclusion about the role of serum copper levels in ATP7A localization in kidneys, we acutely increased serum copper to reach levels that could be more easily interpreted as elevated. Eight-week-old mice were injected intraperitoneally with $CuCl_2$ or with 0.9% NaCl as a control. Four hours after injection, the serum and kidneys were harvested and serum copper concentration and the distribution of ATP7A in tissues were analyzed. The copper-injected animals had a 20-fold higher serum copper concentration than the saline-injected mice ($3{,}769 \pm 181$ and 162 ± 4.5 ppb, respectively). Although copper levels were very high, no obvious adverse effects were

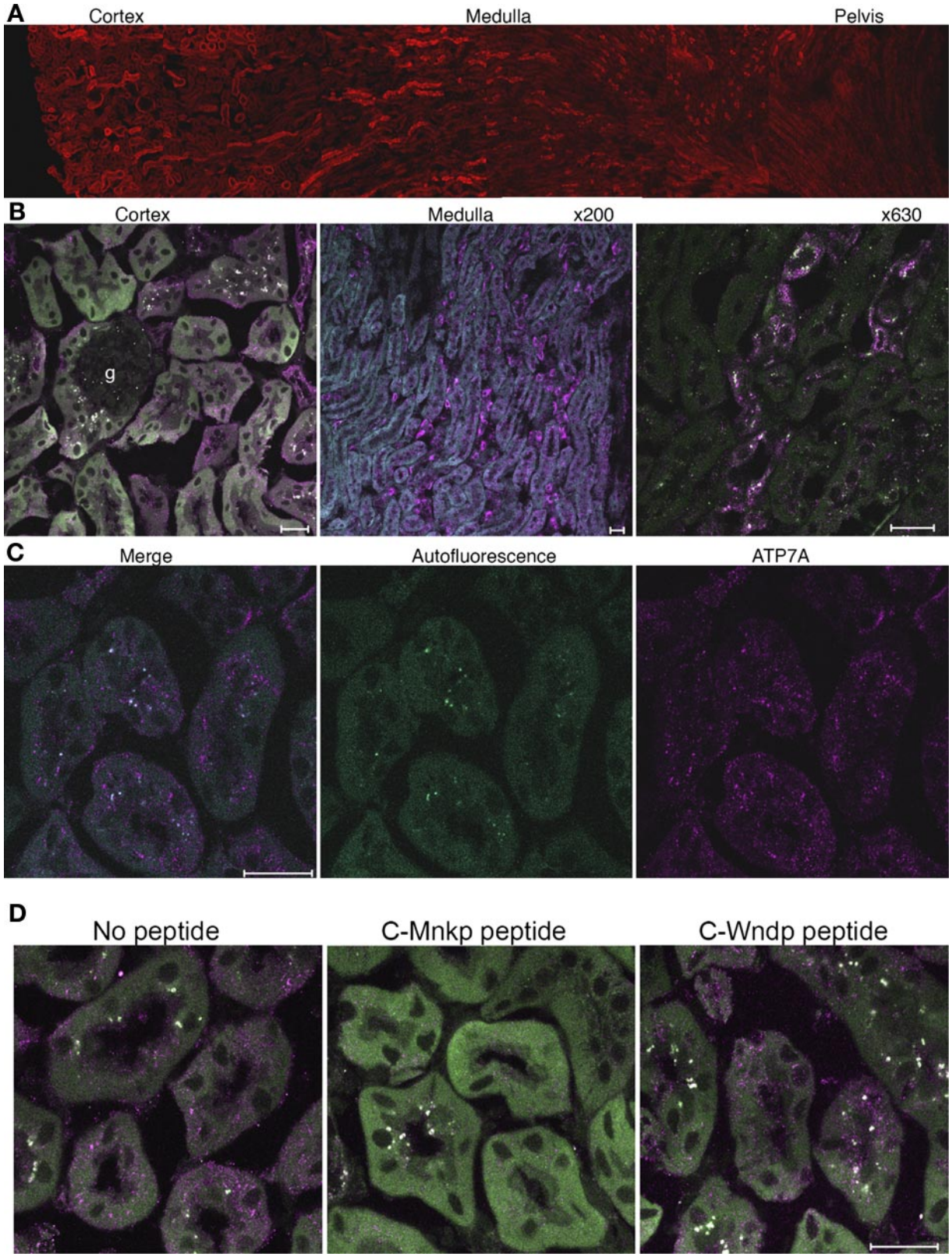

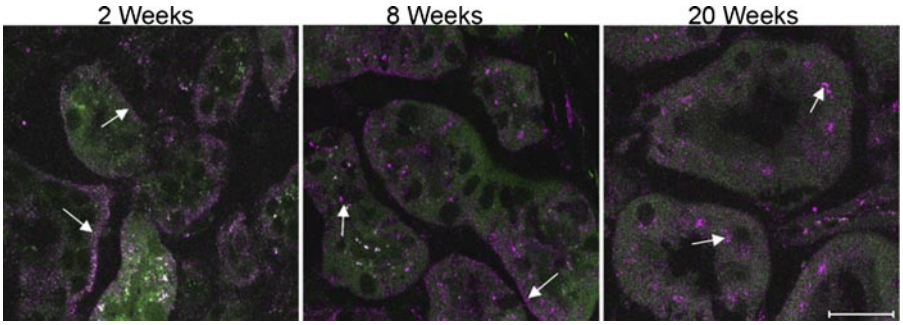

Fig. 2. Intracellular localization of ATP7A in epithelial cells of renal tubules is age dependent. In 2-wk-old kidney, ATP7A is located predominantly at proximity to basolateral membrane. In the cortical tubules of 8-wk-old kidney, ATP7A is seen in both perinuclear and vesicular compartments, and a few tubules exhibit staining close to the basolateral membrane. In the 20-wk-old kidney, ATP7A is located almost entirely in the perinuclear region. ATP7A is shown in pink, autofluorescence in green. Arrows in each panel point to characteristic localization of ATP7A. Scale bar, 20 μm.

observed in the time frame of the experiments. The serum copper concentration of the saline-injected animals was similar to that of noninjected wild-type animals.

In control kidneys, as expected, all mice showed ATP7A staining in the intracellular compartments; however, in many tubules of copper-injected animals, a significant portion of ATP7A was also detected at or near the basolateral membrane (Fig. 4). For a more quantitative comparison, five images from each sample were used to quantify the number of tubules with significant basolateral staining of ATP7A compared with the total number of stained tubules. In saline-injected samples, only 13% (±6.5%) of tubules displayed basolateral ATP7A staining, whereas in samples from copper-injected animals, approximately one-half of the tubules 46% (±7.3%) showed predominant staining in the proximity of the basolateral membrane. Thus endogenous ATP7A traffics in vivo in response to changing copper levels, and elevation of copper in serum can serve as a signal for such relocalization.

ATP7A is expressed in proximal and distal tubular epithelial cells along with ATP7B. In the renal cortex, the majority of tubules correspond to the proximal portion of nephrons, whereas distal tubules account for only a minor fraction of all tubules. Compared with the distribution of the Na-Cl cotransporter NCC, a marker of distal tubules (Supplemental Fig. 1; supplemental data for this article is available online at the *American Journal of Physiology-Renal Physiology* website), the ATP7A staining was far more extensive and, at varying intensities, was seen in almost all tubules (see Fig. 1*A*). To examine whether endogenous ATP7A is present in both proximal and distal tubular epithelial cells, we stained OK and MDCK cells (derived from proximal and distal tubular epithelial cells, respectively) with the anti-ATP7A antibody. These experiments revealed that ATP7A was expressed endogenously in both OK and MDCK cells. In both cell lines under basal conditions, ATP7A was detected in the intracellular perinuclear location consistent with the known TGN localization of ATP7A in other cell lines (Fig. 5).

Previous studies have suggested that another copper-transporting ATPase, ATP7B, is also expressed in kidneys (17, 31) and therefore may contribute to copper homeostasis. Our anti-ATP7B antibody was insufficiently sensitive to detect distribution of ATP7B in tissue of adult mice (although signal was detected in kidney of young animals and in primary cell culture; our data, not shown). Consequently, we examined whether endogenous ATP7B was coexpressed with ATP7A in either OK or MDCK cells. We found that endogenous ATP7B was present in both OK and MDCK cells and, similarly to ATP7A, had intracellular perinuclear localization (Fig. 5).

The intracellular localization of ATP7A is altered in Atp7b$^{-/-}$ *kidney.* The coexpression of two Cu-ATPases in renal cells indicated that both transporters were likely to play a role in balancing renal copper. Our results suggested that ATP7A was likely to export excess copper across the basolateral membrane (see above). To better understand the contribution of ATP7B to renal copper homeostasis, we examined the effects of ATP7B inactivation on renal copper concentration and ATP7A localization using *Atp7b*$^{-/-}$ mice. We hypothesized that in the absence of functional ATP7B, more copper will stay in the cytosol of epithelial cells, thus increasing, to a certain degree, the intracellular copper concentration. In response, ATP7A may traffic toward basolateral membrane to facilitate copper export and compensate for the lack of ATP7B activity. The results of our experiments (Fig. 6) are consistent with this scenario.

Specifically, we observed a very striking change in the intracellular distribution of ATP7A when control and *Atp7b*$^{-/-}$ kidneys were compared. The changes were seen in all *Atp7b*$^{-/-}$ animals but were particularly apparent in older mice. In cortical tubules of 20-wk-old *Atp7b*$^{-/-}$ mice, the majority of ATP7A was located close to the basolateral membrane (Fig. 6*A*, *top*) in contrast to control samples in which most of the ATP7A staining was perinuclear (Fig. 6*A*, *bottom*). Quantitative analysis of images revealed that 68 ± 13% of all tubules in *Atp7b*$^{-/-}$ animals showed predominantly basolateral staining, a higher number than even the copper-injected wild-type samples, which displayed 46 ± 7.3% basolateral staining. The staining in the medulla was predominantly perinuclear, similar to wild-type staining (not shown).

Fig. 1. Localization of the renal copper-transporting ATPase ATP7A in 6- to 8-wk-old kidney. *A*: immunohistochemistry using CT77 antibody revealed bright, abundant staining (red) throughout the kidney cortex and medulla. A sagittal section of kidney is shown. *B*: ATP7A is present in epithelial cells (pink staining) and shows different expression levels along the nephron. In either renal cortex (*left*) or medulla (*middle* and *right*), some tubules display bright ATP7A staining, whereas others show very little staining. This is particularly apparent at high magnification (*right*). The glomerulus (g) is mostly unstained. *C*: specific staining (*right*, pink) can be distinguished from autofluorescence (*middle*, green) with 2-color scanning and image overlay (*left*, autofluorescence appears as white spots). *D*: immunostaining of ATP7A is specific. To determine the specificity of staining, the anti-ATP7A antibody was preincubated with specific (C-Mnkp) and nonspecific (C-Wndp) peptides for 1 h before being added to the slide. Images were taken using the same detector gain and laser intensity. Specific blocking resulted in a significant reduction in staining when C-Mnkp peptide was used, whereas blocking with nonspecific peptide had no effect on ATP7A staining (C-Wndp peptide). ATP7A is shown in pink; autofluorescence in green. Scale bar, 20 μm.

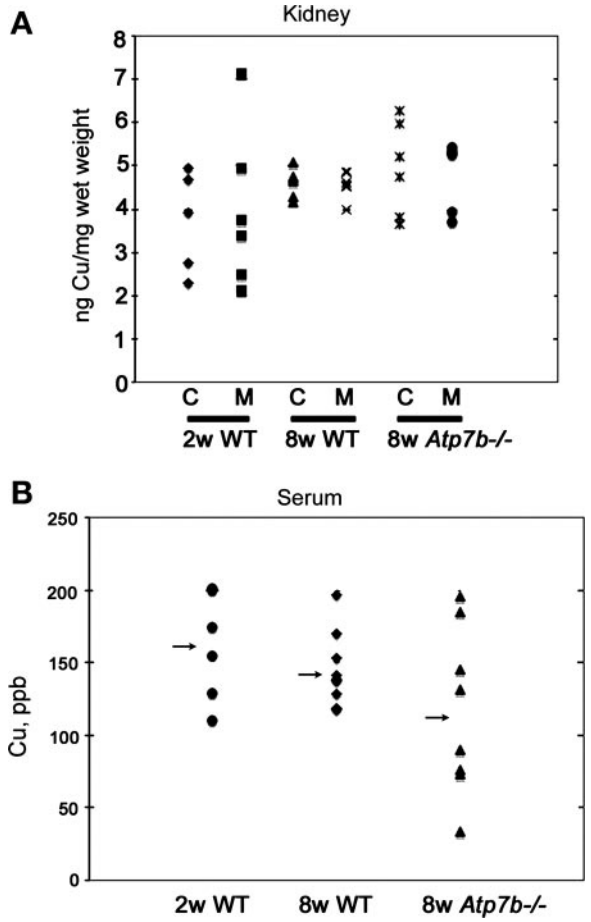

Fig. 3. Copper measurements in tissues and in the serum. Kidneys from 2- and 8-wk-old wild-type (WT) mice and 8-wk-old *Atp7b*$^{-/-}$ mice were dissected into cortex (C) and medulla (M) and were digested and analyzed by atomic absorption spectroscopy for copper content, expressed as ng of copper per mg wet weight. A value for each animal is plotted; $n = 4–6$ animals per condition. *B*: serum measurements for 2- and 8-wk-old WT mice and 8-wk-old *Atp7b*$^{-/-}$ mice. A value for each animal is plotted; $n = 6–9$ animals per condition. Arrows in *B* indicate the mean value for each group.

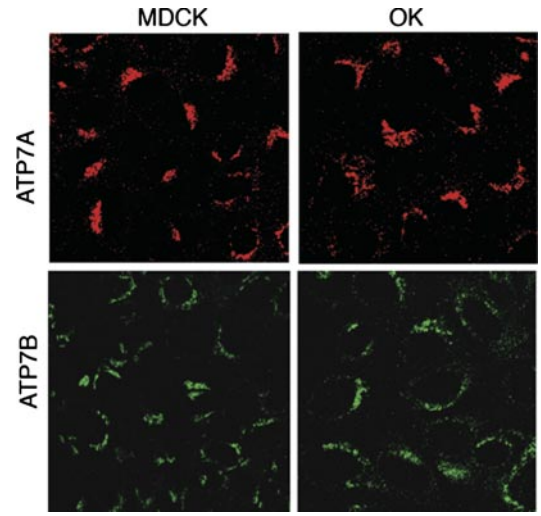

Fig. 4. Localization of endogenous ATP7A and ATP7B in opossum kidney (OK) and Madin-Darby canine kidney (MDCK) cells. Immunostaining with specific antibody CT77 and confocal microscopy illustrated that both ATP7A and ATP7B are endogenously expressed in cells derived from either proximal tubules (OK) or distal tubules (MDCK). The Cu-ATPases show perinuclear localization in both cell types.

Our experiments using wild-type animals indicated that the trafficking of ATP7A in kidney could be induced by changes in serum copper concentration (see above). Consequently, it was important to verify that the changes in the intracellular localization of ATP7A in *Atp7b*$^{-/-}$ *mice* were not due to elevated copper in a serum, which could be an indirect effect of ATP7B inactivation in other tissues. Copper measurements showed that serum copper concentration of the 8-wk-old *Atp7b*$^{-/-}$ animals was not elevated compared with the 8-wk-old wild-type animals (116.31 ± 57.68 ppb in the knockouts compared with 144.61 ± 25.59 ppb in the wild type, Fig. 3*B*).

ATP7A partially compensates for the lack of ATP7B function. In the liver, where ATP7B is the major copper exporter (ATP7A is not expressed in hepatocytes), inactivation of ATP7B is associated with a large (~20-fold higher than the norm) increase in copper content (4, 8). Consequently, it was interesting to determine the levels of copper in the *Atp7b*$^{-/-}$ kidney, where ATP7A relocalized to the basolateral membrane (see above), presumably to export copper. Atomic absorption measurements of copper in kidneys of 8-wk-old control and *Atp7b*$^{-/-}$ mice showed no significant copper accumulation at this stage (Fig. 3*A*). Concentration of copper in cortex and medulla of *Atp7b*$^{-/-}$ mice was comparable to copper concentration in the corresponding regions of the wild-type mice (4.95 ± 1.08 vs. 4.59 ± 0.34 ppb for cortex and 4.71 ± 0.83 vs. 4.57 ± 0.32 ppb for medulla) (Fig. 3).

The lack of significant copper increase in *Atp7b*$^{-/-}$ kidneys suggested that ATP7A compensates for the absence of transport activity of ATP7B. However, this compensation is incomplete, and the kidney metabolism is altered. This was evident from the accumulation of bright fluorescent material, which was present endogenously and was unrelated to immunostaining (Fig. 6*B*, *top*). No such fluorescence was seen in control kidney (Fig. 6*B*, *bottom*). This material concentrated in a fairly narrow zone of the outer medulla of *Atp7b*$^{-/-}$ kidney and showed yellow-orange fluorescence under UV light (360 nm). Similar yellow-orange fluorescence was previously observed in kidneys of Lon-Evans cinnamon (LEC) rats (which also lack

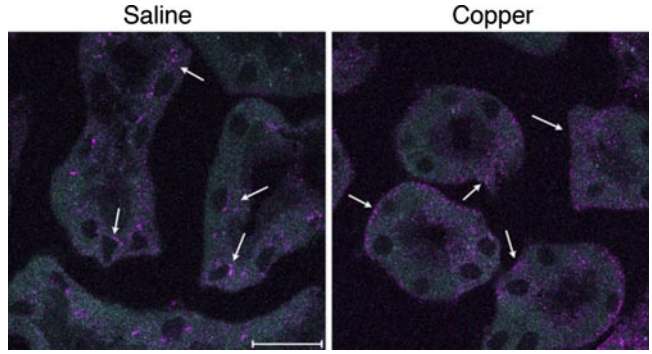

Fig. 5. Elevated copper in serum induces trafficking of ATP7A in vivo. Mice were injected with 0.9% saline (*left*) or with $CuCl_2$ (10 μg Cu/g body wt) solution (*right*), and localization of ATP7A in kidney was characterized by immunostaining with CT77 antibody. ATP7A is shown in pink; arrows indicate areas of predominant localization of ATP7A. Copper injections resulted in a higher proportion of basolateral ATP7A staining, whereas saline injections resulted in the normal, mostly perinuclear distribution and some vesicular staining. Scale bar, 20 μm.

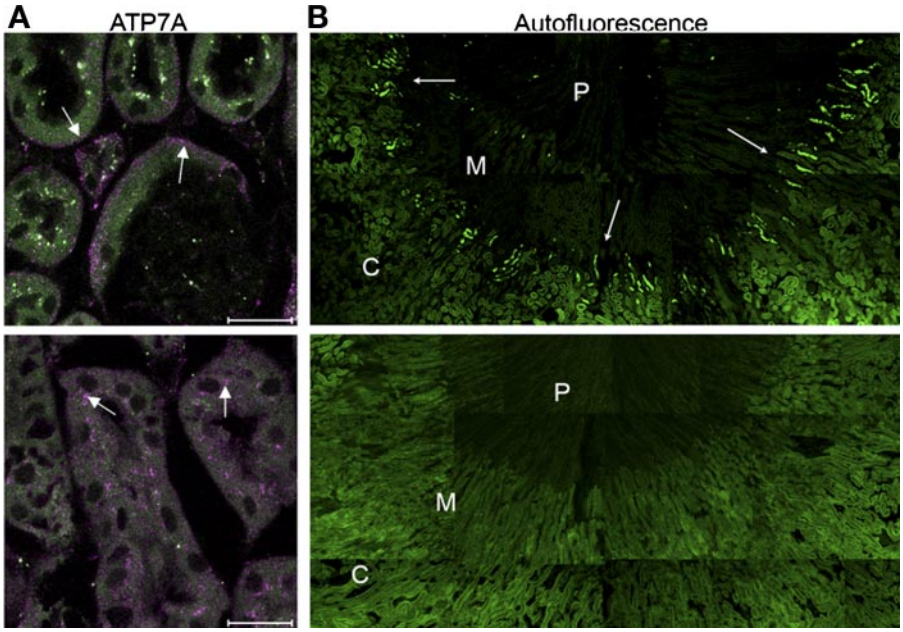

Fig. 6. Metabolic changes and relocalization of ATP7A in kidney lacking functional ATP7B. *A*: immunostaining of ATP7A in *Atp7b*$^{-/-}$ (*top*) and control kidney (*bottom*). In the absence of functional ATP7B, ATP7A was detected in the proximity of the basolateral membrane (*top*), in contrast to the vesicular and *trans*-Golgi network-like staining shown in WT mice (*bottom*). ATP7A is shown in pink; autofluorescence in green. Scale bar, 20 μm. *B*: deposits of intensely fluorescent material, indicated by arrows, are evident in the outer medulla of *Atp7b*$^{-/-}$ kidney (*top*). These deposits are not present in WT mice (*bottom*). To generate an overview of the area, the set of high resolution images were taken in succession and then assembled. C, cortex; M, medulla; P, renal pelvis.

functional ATP7B) and was ascribed to the presence of a copper-metallothionein (Cu-MT) complex (25). In *Atp7b*$^{-/-}$ kidneys, however, the accumulated material also fluoresced under longer wavelengths (up to 630 nm), suggesting that the increased autofluorescence was due to regional accumulation of more than one metabolite.

DISCUSSION

Kidneys show a tight control of their copper content under conditions of either copper deficiency or copper accumulation. We have demonstrated that renal cells coexpress two copper-transporting ATPases, ATP7A and ATP7B, that work together to maintain copper balance within this tissue. The ability of ATP7A to traffic to basolateral membrane (an event associated with copper export) in response to copper elevation strongly suggests that ATP7A plays the major role in exporting copper from renal cells for reabsorption into the blood and in protecting renal cells against copper overload. Consistent with this role, ATP7A is widely expressed throughout the kidney and is present, at various levels, in most tubules. ATP7B is also involved in maintaining intracellular copper levels, likely through the sequestration of excess copper into the vesicles, although a role for ATP7B in the apical export of copper cannot be presently excluded.

The wider distribution of ATP7A observed in our studies compared with previous reports can be explained by the utilization of a more sensitive antibody and fluorescent detection, which further increases sensitivity compared with previously used color detection. Our data agree with the studies reporting high ATP7A expression in cortical tubules and not in the glomerulus (6, 9, 19). It should be noted, however, that the tubules adjacent to glomeruli are brightly stained, and therefore, at low magnification, the characteristic morphology of the Bowman's capsule and proximal convoluted tubule surrounding the glomerulus is easily discernable.

Our experiments using high-magnification confocal imaging yielded additional information on intracellular localization of ATP7A in different tubules. Within the medulla, ATP7A is found almost entirely in the perinuclear region of epithelial cells, in contrast to the perinuclear, vesicular, and basolateral staining seen in the cortex. Previous studies in polarized and nonpolarized cells demonstrated that trafficking of ATP7A from the perinuclear region toward the plasma membrane occurs when extracellular copper is elevated and results in copper export from the cell (5, 13, 24, 27). Therefore, the predominance of ATP7A staining in the perinuclear region of cells in the medulla compared with the cortex may reflect a gradient of extracellular copper along the nephron and/or a low amount of copper export and reabsorption in the loops of Henle compared with that in proximal and distal tubules of the cortex. Similarly, the cortical tubules that exhibit the most basolateral staining are probably those involved in the majority of copper transport from the kidney back into circulation.

Because of the lack of convenient marker antibodies that could be used for colocalization with CT77 (non-rabbit and non-mouse), the precise identity of regions with different localization patterns of ATP7A remains to be determined. However, copper injection experiments illustrate that renal ATP7A relocalizes in vivo and that ATP7A traffics toward the basolateral membrane not only in tubules, where some basolateral staining was already present, but also in other tubules (as evidenced by a significant, up to 50%, increase in the number of tubules with basolateral location of ATP7A). This observation suggests that copper reabsorption into the circulation via ATP7A can occur, when necessary, along a large portion of the nephron; however, under normal conditions, only a very small fraction of the renal tubules is involved in this process.

The experiments in mice of different age demonstrated, for the first time, that the relocalization of ATP7A in vivo also occurs in response to physiological changes that accompany kidney maturation. The large difference in localization of renal ATP7A in 2-wk-old mice (mostly basolateral) and 20-wk-old mice (mostly perinuclear) is unrelated to cortical copper con-

centration, which is clearly not elevated in younger mice. Our analysis of serum, however, cannot exclude the possibility that younger animals have slightly higher copper levels in the serum or that these levels fluctuate more than in adult animals. In cultured cells, the increase of copper in the medium as low as 1 μM triggers relocalization of endogenous ATP7A toward the plasma membrane (24), whereas in animals, the large animal-to-animal variation prevents detection of such small changes. The robust trafficking of renal ATP7A in response to acute copper elevation is consistent with the role of serum copper in altering the ATP7A localization. In addition to regulation by changing copper levels, hormonal regulation of ATP7A trafficking was recently described in placental and mammary cells (7, 10). No information is currently available about hormonal control of renal copper homeostasis; therefore, one cannot exclude the possibility that the localization and function of ATP7A in the kidney can also be modulated by factors other than fluctuations in serum copper levels. If ATP7A localization indeed parallels the copper-export activity of ATP7A, then one would predict that young mice have higher levels of copper reabsorption in the cortex and that this transport decreases with age.

In LEC rats, which lack functional ATP7B, excess copper bound to metallothionein (Cu-MT) was observed in the outer medulla and, to a lesser extent, in the in proximal convoluted tubule cells (25). In contrast, in macular mice, which have impaired ATP7A, Cu-MT was seen only in the cells of proximal convoluted tubules (30, 32). These early results point to an important involvement of both ATP7A and ATP7B in copper homeostasis in proximal tubules. The marked change in the intracellular localization of ATP7A that we observed in the cortical tubules of *Atp7b*$^{-/-}$ mice complements the earlier data and strongly supports this conclusion.

Altogether, the data are consistent with a role for ATP7A in the transport of copper across the basolateral membrane and, hence, in copper reabsorption into the blood. The copper injection experiments indicate that it is renal ATP7A that responds to short-term serum copper fluctuations. We suggest that ATP7A, which shows faster kinetics properties than ATP7B (2), works as a housekeeping copper transporter and provides fast response to elevated copper by trafficking to renal basolateral membrane. Inactivation of ATP7A would prevent export of copper from the tubules resulting in copper accumulation.

The role of renal ATP7B appears to be to fine-tune the intracellular copper concentration, likely by transporting copper into intracellular vesicles. Our data suggest that inactivation of ATP7B may cause local changes in copper concentrations that trigger trafficking of ATP7A toward plasma membrane for the restoration of copper balance. Thus the export of excess copper by ATP7A is one of the likely reasons for a very slow copper accumulation by *Atp7b*$^{-/-}$ kidneys. Although this explanation is consistent with a greatly increased basolateral localization of ATP7A in *Atp7b*$^{-/-}$ mice, more complex systemic effects of ATP7B inactivation on kidney cannot be excluded. Development of tissue-specific knockouts would greatly facilitate understanding of tissue-specific functions for Cu-ATPases.

The absence of functional ATP7B in *Atp7b*$^{-/-}$ mice also leads to the appearance of fluorescent deposits in the outer medulla. Interestingly, the observed pattern of increased autofluorescence in the narrow region of outer medulla is similar to the pattern of Cu-MT fluorescence seen in LEC rats (25) (see above). However, the fluorescence characteristics differ in *Atp7b*$^{-/-}$ mice and LEC rats. The fluorescent material in the *Atp7b*$^{-/-}$ mice is excited at UV (360 nm) and longer wavelengths (up to 630 nm), suggesting that, in our case, it represents a mixture of substances, possibly including lipofuscin. Lipofuscin is a fluorescent pigment that has a broad absorption and excitation spectrum, and it progressively accumulates as a result of autophagocytosis of modified molecules within secondary lysosomes. Lipofuscin particles containing accumulated copper were previously observed in the liver of Wilson disease patients (18). In *Atp7b*$^{-/-}$ mice, similar accumulation of lipofuscin-like material occurs in a specific kidney region, suggesting that this is the region where the function of ATP7B is particularly important.

ACKNOWLEDGMENTS

We thank Dr. David H. Ellison for the kind gift of anti-NCC antibody and helpful discussions. We thank Tony Capps for performing copper measurements.

GRANTS

This work was supported by National Institutes of Health grants PO1 GM 067166-01 to S. Lutsenko and J. H. Kaplan and DK-32949 to B. Eipper.

REFERENCES

1. **Allen KJ, Buck NE, Cheah DM, Gazeas S, Bhathal P, Mercer JF.** Chronological changes in tissue copper, zinc and iron in the toxic milk mouse and effects of copper loading. *Biometals* 19: 555–564, 2006.
2. **Barnes N, Tsivkovskii R, Tsivkovskaia N, Lutsenko S.** The copper-transporting ATPases, Menkes and Wilson disease proteins, have distinct roles in adult and developing cerebellum. *J Biol Chem* 280: 9640–9645, 2005.
3. **Bearn AG.** Wilson's disease. *Am J Clin Nutr* 9: 695–699, 1961.
4. **Buiakova OI, Xu J, Lutsenko S, Zeitlin S, Das K, Das S, Ross BM, Mekios C, Scheinberg H, Gilliam CT.** Null mutation of the murine *ATP7B* (Wilson disease) gene results in intracellular copper accumulation and late-onset hepatic nodular formation. *Hum Mol Genet* 8: 1665–1671, 1999.
5. **Greenough M, Pase L, Voskoboinik I, Petris MJ, Wilson O'Brien A, Camakaris J.** Signals regulating trafficking of Menkes (MNK; ATP7A) copper-translocating P-type ATPase in polarized MDCK cells. *Am J Physiol Cell Physiol* 287: C1463–C1471, 2004.
6. **Grimes A, Hearn CJ, Lockhart P, Newgreen DF, Mercer JFB.** Molecular basis of the brindled mouse mutant (*Mo^{br}*): a murine model of Menkes disease. *Hum Mol Genet* 6: 1037–1042, 1997.
7. **Hardman B, Michalczyk A, Greenough M, Camakaris J, Mercer JFB, Ackland ML.** Hormonal regulation of the Menkes and Wilson copper-transporting ATPases in human placental Jeg-3 cells. *Biochem J* 402: 241–250, 2007.
8. **Huster D, Finegold MJ, Morgan CT, Burkhead JL, Nixon R, Vanderwerf SM, Gilliam TC, Lutsenko S.** Consequences of copper accumulation in the livers of the Atp7b$^{-/-}$ (Wilson disease gene) knockout mice. *Am J Pathol* 168: 423–434, 2006.
9. **Ke BX, Llanos RM, Wright M, Deal Y, Mercer JFB.** Alteration of copper physiology in mice overexpressing the human Menkes protein ATP7A. *Am J Physiol Regul Integr Comp Physiol* 290: R1460–R1467, 2006.
10. **Kelleher SL, Lönnerdal B.** Mammary gland copper transport is stimulated by prolactin through alterations in Ctr1 and Atp7A localization. *Am J Physiol Regul Integr Comp Physiol* 291: R1181–R1191, 2006.
11. **Kodama H, Abe T, Takama M, Takahashi I, Kodama M, Nishimura M.** Histochemical localization of copper in the intestine and kidney of macular mice: light and electron microscopic study. *J Histochem Cytochem* 41: 1529–1535, 1993.
12. **Kurasaki M, Okabe M, Saito S, Suzuki-Kurasaki M.** Copper metabolism in the kidney of rats administered copper and copper-metallothionein. *Am J Physiol Renal Physiol* 274: F783–F790, 1998.

13. **La Fontaine S, Firth SD, Camakaris J, Englezou A, Theophilos MB, Petris MJ, Howie M, Lockhart PJ, Greenough M, Brooks H, Reddel RR, Mercer JFB.** Correction of the copper transport defect of Menkes patient fibroblasts by expression of the Menkes and Wilson ATPases. *J Biol Chem* 273: 31375–31380, 1998.
14. **La Fontaine S, Mercer JFB.** Trafficking of the copper-ATPases, ATP7A and ATP7B: role in copper homeostasis. *Arch Biochem Biophys* 463: 149–167, 2007.
15. **Linder MC, Hazegh-Azam M.** Copper biochemistry and molecular biology. *Am J Clin Nutr* 63: 797S–811S, 1996.
16. **Monty JF, Llanos RM, Mercer JFB, Kramer DR.** Copper exposure induces trafficking of Menkes protein in intestinal epithelium of ATP7A transgenic mice. *J Nutr* 135: 2762–2766, 2005.
17. **Moore SDP, Cox DW.** Expression in mouse kidney of membrane copper transporters Atp7a and Atp7b. *Nephron* 92: 629–634, 2002.
18. **Motonishi S, Hayashi H, Fujita Y, Okada H, Kusakabe A, Ito M, Miyamoto K, Ueno T.** Copper- and iron-rich matrices in hepatocellular lipofuscin particles of a young male patient: diagnostic ultrastructures for Wilson disease. *Ultrastruct Pathol* 30: 409–414, 2006.
19. **Murata Y, Kodama H, Abe T, Ishida N, Nishimura M, Levinson B, Gitschier J, Packman S.** Mutation analysis and expression of the mottled gene in the macular mouse model of Menkes disease. *Pediatr Res* 42: 436–442, 1997.
20. **Niciu MJ, Ma XM, El Meskini R, Ronnett GV, Mains RE, Eipper BA.** Developmental changes in the expression of ATP7A during a critical period in postnatal neurodevelopment. *Neuroscience* 139: 947–964, 2006.
21. **Nomiyama K, Nomiyama H, Kameda N, Tsuji A, Sakurai H.** Mechanism of hepatorenal syndrome in rats of Long-Evans Cinnamon strain, an animal model of fulminant Wilson's disease. *Toxicology* 132: 201–214, 1999.
22. **Nooijen JL, De Groot CJ, Van den Hamer CJ, Monnens LA, Willemse J, Niermeijer MF.** Trace element studies in three patients and a fetus with Menkes' disease. Effect of copper therapy. *Pediatr Res* 15: 284–289, 1981.
23. **Nose Y, Kim BE, Thiele DJ.** Ctr1 drives intestinal copper absorption and is essential for growth, iron metabolism, and neonatal cardiac function. *Cell Metab* 4: 235–244, 2006.
24. **Nyasae L, Bustos R, Braiterman L, Eipper B, Hubbard A.** Dynamics of endogenous ATP7A (Menkes protein) in intestinal epithelial cells: copper-dependent redistribution between two intracellular sites. *Am J Physiol Gastrointest Liver Physiol* 292: G1181–G1194, 2007.
25. **Okabe M, Nakayama K, Kurasaki M, Yamasaki F, Aoyagi K, Yamanoshita O, Sato S, Okui T, Ohyama T, Kasai N.** Direct visualization of copper-metallothionein in LEC rat kidneys: application of autofluorescence signal of copper-thiolate cluster. *J Histochem Cytochem* 44: 865–873, 1996.
26. **Parker MM, Humoller FL, Mahler DJ.** Determination of Copper and Zinc in Biological Material. *Clin Chem* 13: 40–48, 1967.
27. **Pase L, Voskoboinik I, Greenough M, Camakaris J.** Copper stimulates trafficking of a distinct pool of the Menkes copper ATPase (ATP7A) to the plasma membrane and diverts it into a rapid recycling pool. *Biochem J* 378: 1031–1037, 2004.
28. **Prohaska JR.** Changes in tissue growth, concentrations of copper, iron, cytochrome oxidase and superoxide dismutase subsequent to dietary or genetic copper deficiency in mice. *J Nutr* 113: 2148–2158, 1983.
29. **Steveson TC, Ciccotosto GD, Ma XM, Mueller GP, Mains RE, Eipper BA.** Menkes protein contributes to the function of peptidylglycine alpha-amidating monooxygenase. *Endocrinology* 144: 188–200, 2003.
30. **Suzuki-Kurasaki M, Okabe M, Kurasaki M.** Copper-metallothionein in the kidney of macular mice: a model for Menkes disease. *J Histochem Cytochem* 45: 1493–1501, 1997.
31. **Tanzi RE, Petrukhin K, Chernov I, Pellequer JL, Wasco W, Ross B, Romano DM, Parano E, Pavone L, Brzustowicz LM, Devoto M, Peppercorn J, Bush AI, Sternlieb I, Pirastu M, Gusella JF, Evgrafov O, Penchaszadah GK, Honig B, Edelman IS, Soares MB, Scheinberg IH, Gilliam TC.** The Wilson disease gene is a copper transporting ATPase with homology to the Menkes disease gene. *Nat Genet* 5: 344–350, 1993.
32. **Yoshimura N.** Histochemical localization of copper in various organs of brindled mice. *Pathol Int* 44: 14–19, 1994.